

## DEVELOPMENT OF A MAGNETICALLY SUSPENDED, TETRAHEDRON-SHAPED ANTENNA POINTING SYSTEM

Kenichi Takahara\*, Tamane Ozawa\*, Hiroshi Takahashi\*,  
Shitta Shingu\*, Toshiro Ohashi\*\*, Hitoshi Sugiura\*\*

### ABSTRACT

A magnetically suspended, tetrahedron-shaped antenna pointing system is proposed for use in a multibeam broadcasting satellite system in the future. This paper presents the structure of this system, its design concept and the functional test results which were obtained in a laser tracking system in the laboratory. According to these results, it has been confirmed that the system has many advantages over conventional systems and excellent performance.

### INTRODUCTION

Satellite broadcasting, which aims at regional services such as high definition television and digital television, is planned in the near future in Japan using 22 GHz-band beams. In one of the plans for this broadcasting system, Japan will be served with 6 precision beams for regional broadcasting as shown in Fig. 1 (ref. 1).

Whereas the distance between a geostationary satellite and the earth is about 36000 km, the attitude control error (0.1 degree in conventional control methods for a satellite stabilized in three axes) corresponds to about 60 km distance on the earth. In order to realize an effective regional broadcasting system, this corresponding distance should be less than 6 km on the earth. Accordingly, the required pointing error for the antenna system is less than 0.01 degree. An offset Cassegrain antenna consisting of a main reflector, a sub reflector, and horns will be mounted in the satellite antenna system shown in Fig. 2. Since the main reflector is fixed to the satellite body, directly driving this large reflector is almost impossible. Rather, the small sized sub reflector must be driven by an Antenna Pointing Mechanism (APM). By driving the sub reflector to compensate for the satellite perturbation movement, the transmitted and received electric waves will be correctly directed to Japan in conformity with the RF beacon from the earth station.

In conventional APMs, lubricated ball bearings or flexible pivots are used (refs. 2 and 3). On the other hand, an APM using magnetic suspension has

---

Toshiba Corporation, Kawasaki, Japan

\* Research and Development Center, Mechanical Engineering Laboratory

\*\* Komukai Works, Space Programs Division

PRECEDING PAGE BLANK NOT FILMED

such advantages as no wear, no friction and no lubrication requirement (ref. 4). For this application, the magnetically suspended, tetrahedron-shaped APM (T-MAPS: Toshiba type Magnetically Suspended Antenna Pointing System) is proposed. The important feature of the T-MAPS is the use of a tetrahedral armature. Because of the simplicity of the tetrahedron, the T-MAPS is able to drive the armature contactlessly in 6 degrees of freedom and is therefore clearly superior to other mechanical APMs. The T-MAPS has demonstrated a 0.002 degree pointing accuracy during laboratory tracking tests utilizing a laser beam.

#### REQUIREMENT

According to the plan for the satellite broadcasting system, aperture diameters for the main and sub reflectors are about 3 meters and 0.7 meters respectively.

In the total antenna system, the pointing error based on RF sensor signals should be less than 0.01 degree. However the required pointing accuracy for the T-MAPS, which drives the sub reflector with 0.7 kg·m<sup>2</sup> moment of inertia and 2.0 kg mass, is 0.002 degree. The pointing ranges required are +1.5 degrees which includes satellite movements and misalignment between the antennas and the satellite body. Specified power consumption is less than 0.2 W in orbit.

Mechanical life is expected to be virtually infinite. Life limiting items are limited to electronic devices.

#### DESIGN CONCEPT

##### REDUCTION IN NUMBER OF ELECTROMAGNETS

For the previously manufactured 6 degree-of-freedom APM, it was necessary to use more than 12 electromagnets, because the electromagnets exerted only a pull force. The mechanism was very complicated, requiring a large number of displacement sensors and electromagnets. Furthermore, it became too heavy to be practical in a flight model. In the redesigned APM, the authors carefully considered a reduction in the number of electromagnets and arrived at the tetrahedron configuration. The tetrahedron is a most simple geometric shape and is nonorthogonal. Using these factors, the 12 active electromagnets were reduced to 9 without any functional loss. Consequently, reduced weight and increased reliability were obtained.

##### REDUNDANCY

Though an electromagnet generates only a pull force in one direction, a displacement sensor is available in both plus and minus directions. Therefore, essentially only 6 sensors are required. Accordingly, even in the case of damage to any of the three sensors, the T-MAPS maintains normal operation by changing the sensor signal processing algorithm.

Similarly, the minimum number of electromagnets required to maintain freedom positioning is 7. Therefore, the T-MAPS with 9 electromagnets has redundant actuation capability.

#### MECHANISM DESCRIPTION

The T-MAPS is illustrated in Fig. 3. Fig. 4 shows a photograph, illustrating the sub reflector fixed to the mechanism. The T-MAPS consists of a tetrahedral armature fixed to a support shaft, 9 electromagnets, 9 eddy current displacement sensors, several support members and a base. The sub reflector will be fixed to the top of the support shaft. Nine electromagnet and sensor units are placed so that 3 units are attached to the top face of the armature, and 6 units attach to 3 side faces. Each electromagnet consists of a horseshoe-shaped ferromagnetic material with coils wound around the yoke. The armature is enclosed inside 4 support members, to which each electromagnet and sensor unit is fixed. The clearance gap between individual magnet units and the armature corresponds to the pointing range for the T-MAPS. Consequently, the T-MAPS is simpler than any other mechanical APM.

On the other hand, the T-MAPS requires two special considerations with regard to its control method, due to adopting the tetrahedron and the electromagnet units, as described later.

The specifications for the T-MAPS are shown in Table 1.

Since the T-MAPS is a bread board model, a launch lock device, thermal protection (if needed) and other special equipment suited to space environment have not been built. However, these technologies are already established, so the T-MAPS can easily be converted into a flight model with conventional technologies. Similarly, it is expected that the mechanism and its drive electronics will be substantially lightened for the flight units.

#### MAGNETIC SUSPENSION CONTROL SYSTEM

##### CONTROLLER DESCRIPTION

The magnetic suspension control system is shown in Fig. 5. In this servo control system, each electromagnet is independently controlled by an individual analog PD controller in a local coordinate system with each electromagnet. The displacements between the armature and the sensors are detected by each sensor. These signals are then fed back to compensators. In this control block diagram, there are two special transformers which need careful treatment. One is a command transformation matrix,  $R$ , in which commands in a Cartesian coordinate system are transformed into local commands in local (actuator) coordinates. The other is a position transformation matrix,  $P$ , in which displacement signals of each sensor are transformed into displacement signals in the local (actuator) coordinates.

## COMMAND TRANSFORMATION

Six independent commands, which determine the armature position, are described in vector form by  $C$  ( $c_1, \dots, c_9$ ) and the displacement vectors perpendicular to the plane, which a magnetic force operates on, are described by  $A$  ( $a_1, \dots, a_9$ ). The relationship between the commands and the displacements is as follows:

$$A = F_1(C) \quad (1)$$

where  $F_1$  is a high order vector function which is geometrically obtained from the armature dimensions, electromagnet arrangement and magnetic force vector directions. In practice, the command transformation circuits should be as simple as possible. So applying the linear approximation around the center of the pointing ranges, the eq. (1) becomes:

$$\Delta A = R \cdot C \quad (2)$$

where  $R$  is a command transformation matrix, which is obtained from the mathematical model under the above geometrical conditions.

## POSITION TRANSFORMATION

Similarly to the previous procedure, displacement vectors perpendicular to the sensor positions are described by  $S$  ( $s_1, \dots, s_9$ ). The relational equation between  $C$  and  $S$  is shown as:

$$S = F_2(C) \quad (3)$$

where  $F_2$  is another vector function. Applying the linear approximation to the eq. (3), the following relationship is obtained.

$$\Delta S = D \cdot \Delta C \quad (4)$$

Eliminating  $\Delta C$  using eqs. (2) and (4), the instant transformation matrix,  $P$ , with which sensor position displacements can be transformed into operating force point displacements, will be obtained. However, the transformation matrix,  $D$ , does not have an inverse, because  $\Delta A$  and  $\Delta S$  differ from  $\Delta C$  in matrix order.

Therefore, using the method of least squares, the position transformation matrix  $P$  is finally obtained as follows:

$$A = P \cdot S \quad (5)$$

$$P = R \cdot (D^T \cdot D)^{-1} \cdot D^T \quad (6)$$

where  $D^T$  denotes the transposed matrix for  $D$  and  $(D^T \cdot D)^{-1}$  represents the inverse matrix for  $(D^T \cdot D)$ .

The two transformation matrices,  $R$  and  $P$ , have only constant elements. Accordingly, the transformation calculation involves simple multiplication of matrices, and its analog circuits can be easily constructed.

## PD COMPENSATOR

The transfer function for the PD compensator in the magnetic suspension system is shown in Fig. 6. This figure indicates the typical phase lead-lag compensation. The tetrahedral armature can be stably levitated by use of this PD compensator in all actuator coordinates. In order to suppress excitation over 1 kHz, the gain would be gradually reduced. It was realized, in experiments, that the frequency range for phase lead should be adjusted to the natural frequency of the magnetic suspension system in consideration of mechanical conditions.

## FUNCTIONAL TEST

Functional tests were performed in atmosphere at room temperature, on the following three items:

- (a) Magnetic levitational characteristics.
- (b) Frequency response.
- (c) Resolution.

(a) Using the controller shown in Fig. 5 and adjusting the compensators to magnetically levitate the armature fixed to the sub reflector, it was demonstrated that the system could be stably levitated without a gravity-compensating support. The armature was magnetically levitated in a nominal position by applying a 3 A bias current to each of the 3 electromagnets mounted to the top face of the armature. The magnetic suspension rigidity was 200 N/mm in each of the three lateral directions.

(b) Frequency response for the suspended system was obtained by converting swept sine signals into commands. Test results are shown in Fig. 7. In the z-axis case, the armature precisely tracked the command with no phase lag in the frequency range up to 2 Hz. Similar results were obtained for other axes.

(c) The resolution of the T-MAPS was evaluated by converting micro-rectangular signals into commands. The test results are shown in Fig. 8. In these figures, the upper plot is the input command, and the lower plot shows the signal from the displacement sensor. Jagged signals observed in these figures are natural noises. These figures show that the translational resolution of the armature is less than 0.5  $\mu\text{m}$ . Similarly to the measurement in Fig. 8, the rotational motion resolution is less than  $5 \times 10^{-4}$  degree, as shown in Fig. 9.

## LASER TRACKING SYSTEM

### TEST EQUIPMENT DESCRIPTION

A system using a laser beam instead of an RF beam (see Fig. 10) was constructed to confirm the T-MAPS pointing accuracy. This optical system consisted of a laser generator substituted for a feed horn, a tracking mirror for an antenna, a corner cube reflector for an earth station and a two-dimensional photo detector for an RF sensor.

The corner cube reflector was rotated with some eccentricity. In this test system, the corner cube reflector rotation corresponded to the satellite perturbation movement. In an actual situation, the earth station is fixed and the remaining system components which are mounted on the satellite are moving.

The pointing closed loop, shown in Fig. 11, consisted of PID controllers, the magnetic suspension system described already, and the optical system. This control loop simulated the tracking control for the RF beacon. The deviation between the photo detector outputs and disturbances corresponded to the pointing error. In order to obtain high pointing accuracy, an integral compensator furnished an effective means to obtain the desired characteristics. Ordinarily, integral compensator use not only stabilizes the system, but also decreases the deviation. The disadvantage, however, is that pointing response frequency would be low. However, the 2-ton class satellite considered has a low perturbation motion natural frequency, below 0.1 Hz; therefore integral compensation is sufficiently useful.

As a result, the pointing error, with integral compensation, was virtually zero.

#### LASER TRACKING TEST

In this laser tracking system, when the tracking servo was not working, a circle was drawn on the screen by a laser beam, in accordance with the corner cube reflector rotation with constant eccentricity. The rotation frequency was about 0.1 Hz, as in the case of the satellite movement. For closed-loop operation, a circle was drawn on a two-dimensional semiconductor photo detector.

When the sensed signals from the detector were converted into  $0y$  and  $0z$  commands, the tracking mirror tracked the corner cube reflector and the deviation signals in the controller became virtually zero. At the same time, the laser beam on the screen showed no observable motion.

Fig. 12 shows the  $x$  and  $y$  output signals for the photo detector. In this figure, tracking started at the time corresponding to maximum  $y$  direction value. The pointing accuracy for the T-MAPS was confirmed to be as precise as 0.002 degrees.

Test results, including those from the functional test, are shown in Table 2.

#### CONCLUSIONS

It has been clearly proved that the newly developed T-MAPS is well adapted for multi-beam broadcasting satellite systems. The use of magnetic suspension and a tetrahedral armature offers T-MAPS numerous advantages. These advantages are realized in a concrete manner, as follows.

- (a) High pointing accuracy, 0.002 degree with no wear, no friction, and no lubrication required.

- (b) Low power consumption, less than 0.2 W in orbit except for power consumption in electronics.
- (c) Simple construction and easy manufacturing of electromagnet/displacement sensor units and support members.
- (d) Light weight with a reduction in the number of electromagnets.
- (e) Sensor redundancy, with 9 displacement sensors. (Only 6 sensors are needed.)
- (f) Electromagnetic redundancy, with 9 electromagnets. (7 electromagnets are needed.)
- (g) Reliability, with contactless drive and the above mentioned redundancies.
- (h) High resolution capability; the minimum sensed displacement was less than 0.5  $\mu\text{m}$  in translation, and  $5 \times 10^{-4}$  degrees in rotation.
- (i) Possibility of changing the rotational center, by adjusting misalignments between the satellite body and the antennas, in order to increase the antenna gain.
- (j) Flexible adaption to other applications; for example, jitter isolation mounts, laser communication equipment and other drive mechanisms.

The identification of damaged electromagnets and displacement sensors has been considered.

Improvement and development will be continued until the flight model is completed.

#### REFERENCES

1. S. Yoshimoto, et al., A Trade-Off Study on 22 GHz-Band Multibeam Satellite Broadcasting Systems, AIAA 11th Communication Satellite Systems Conference (1986)
2. H. Heimerdinger, AN ANTENNA POINTING MECHANISM FOR LARGE REFLECTOR ANTENNAS, 15th Aerospace Mechanism Symposium, NASA CP-2181 (1981)
3. B. Hubert and P. Brunet, SOFA: SYSTEME D'ORIENTATION FINE D'ANTENNE, 15th Aerospace Mechanism Symposium, NASA CP-2181 (1981)
4. W. Anderson and S. Joshi, The Annular Suspension and Pointing (ASP) System for Space Experiments and Predicted Pointing Accuracies, NASA TR R-448 (1975)

#### BIBLIOGRAPHY

1. D. Cunningham, et al., Control System Design of the Annular Suspension and Pointing System, J. GUIDANCE AND CONTROL, Vol. 3, No. 1 (1980)
2. S. Iwaki and R. Matsuda, Testing and Investigation of Magnetically Suspended APM, Proceedings of 15th ISTS, Vol. 1 (1986)

Table 1 SPECIFICATIONS

ITEMS	CHARACTERISTICS
DEGREES OF FREEDOM	6
PAYLOAD MOMENT OF INERTIA PAYLOAD MASS	0.7 kg·m <sup>2</sup> 2.0 kg
POINTING RANGE x, y, z θx, θy, θz	±2 mm ±1.5 deg.
ARMATURE MASS	2.1 kg
TOTAL MASS (WITH SUPPORT MEMBERS)	8.0 kg
TOTAL SIZE (WITHOUT PAYLOAD)	□ 250 × 200 mm

Table 2 PERFORMANCE  
(confirmed by laboratory tests)

ITEMS	PERFORMANCE
NATURAL FREQUENCY	4 Hz
COIL WATTAGE ON EARTH IN ORBIT (CALCULATION)	10 W 0.2 W
RESOLUTION TRANSLATION ROTATION	0.5 μm 5 × 10 <sup>-4</sup> deg.
POINTING ACCURACY	0.002 deg.



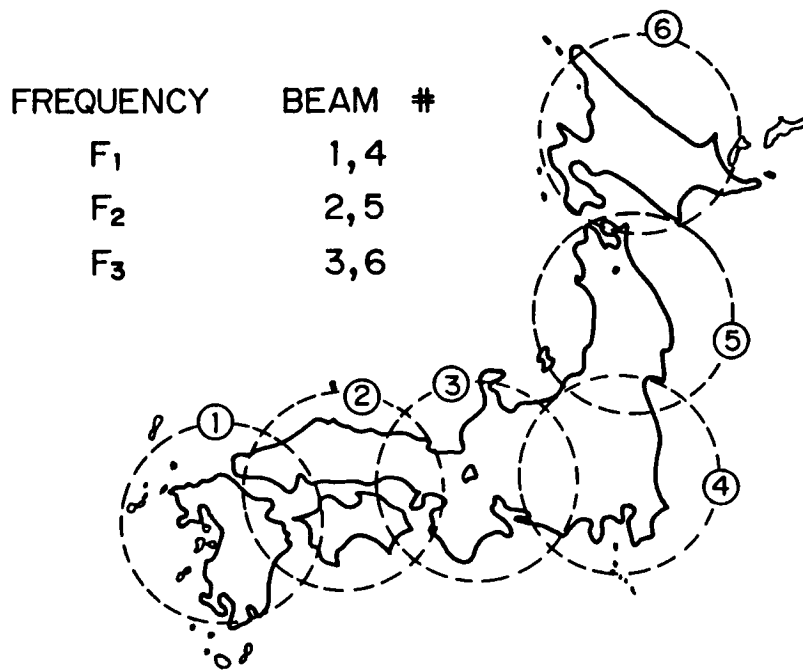


Figure 1 Beam Allotment of Regional Broadcasting for 6 Beams in the Future

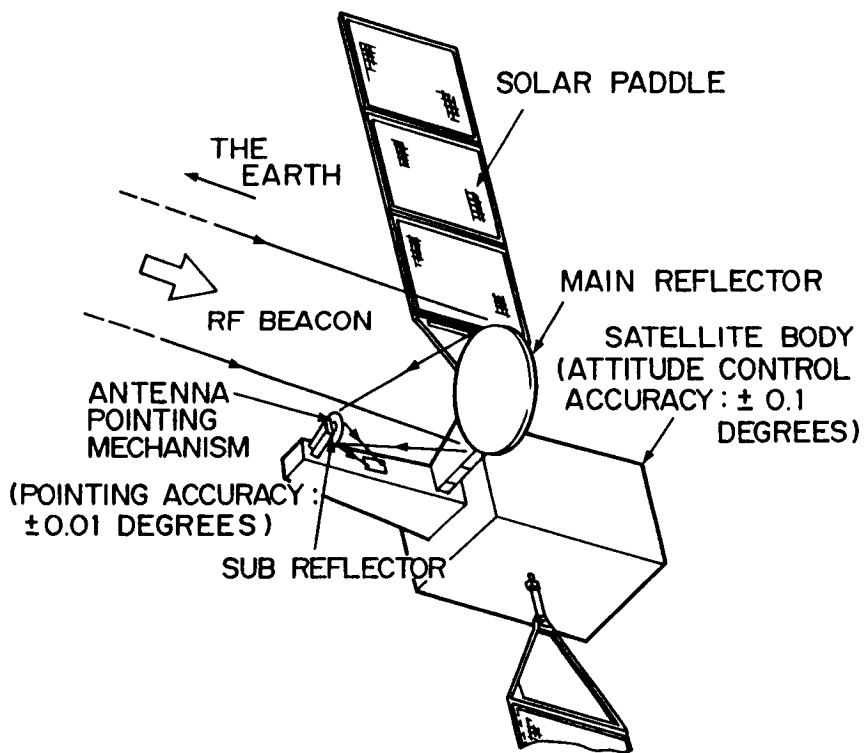


Figure 2 Broadcasting Satellite Antenna System

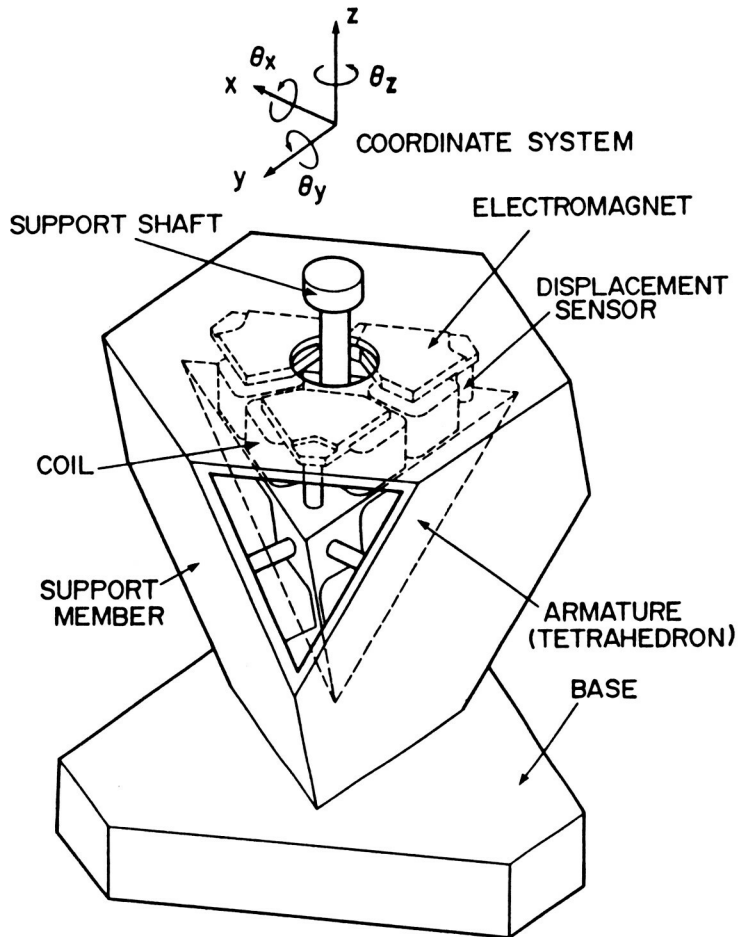


Figure 3 Magnetically Suspended, Tetrahedron-Shaped Antenna Pointing Mechanism

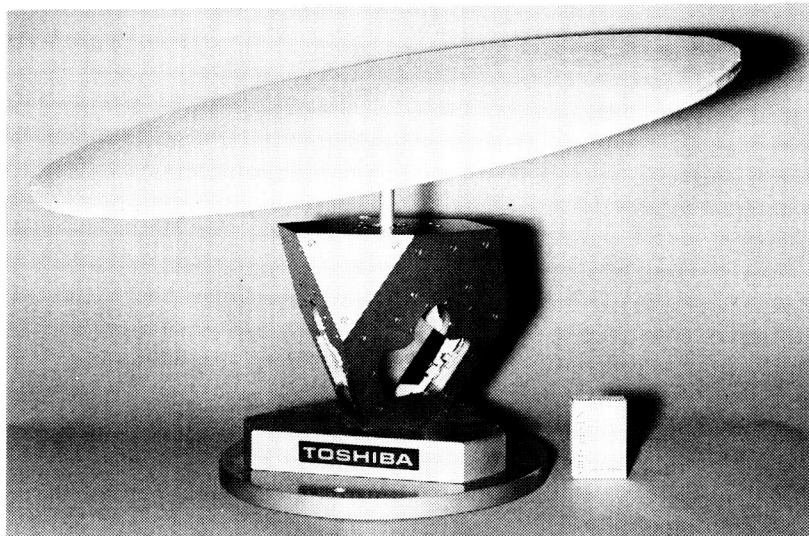


Figure 4 The Mechanism (T-MAPS)

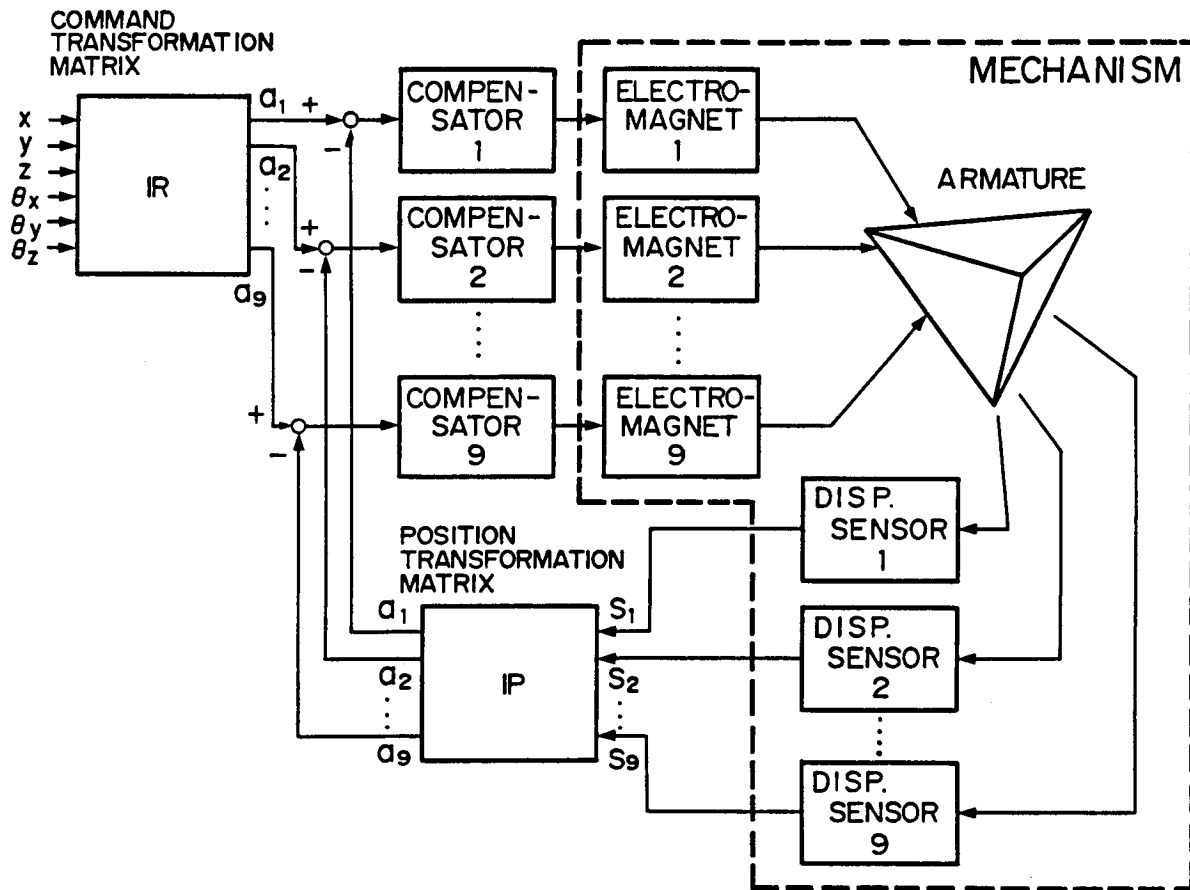


Figure 5 Control Block Diagram for Magnetic Suspension System

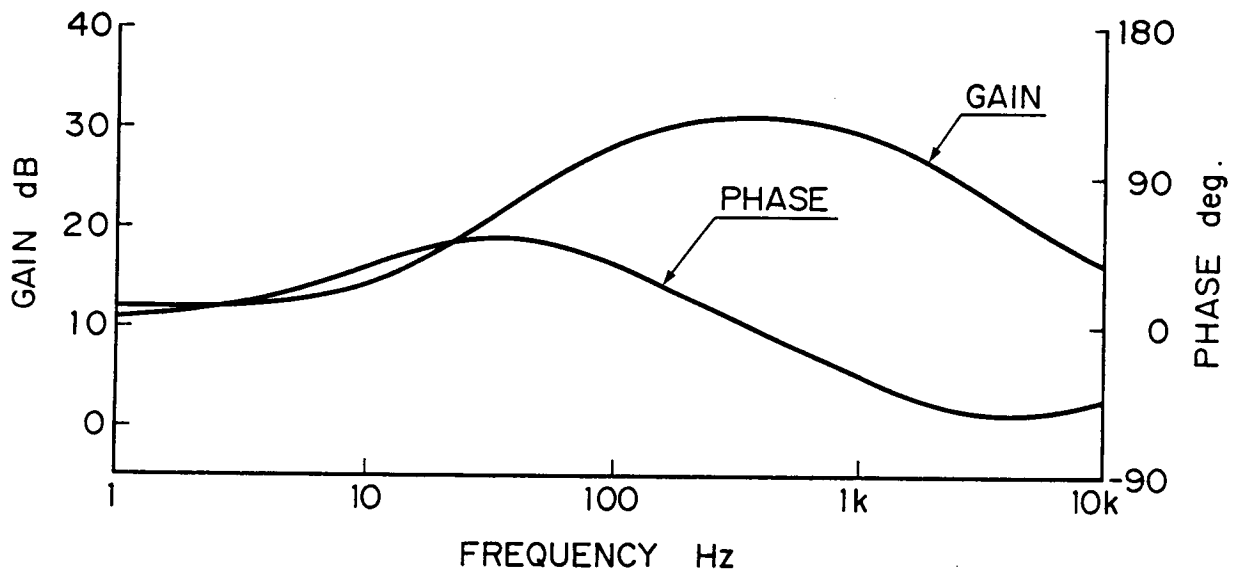


Figure 6 PD Compensator Transfer Function

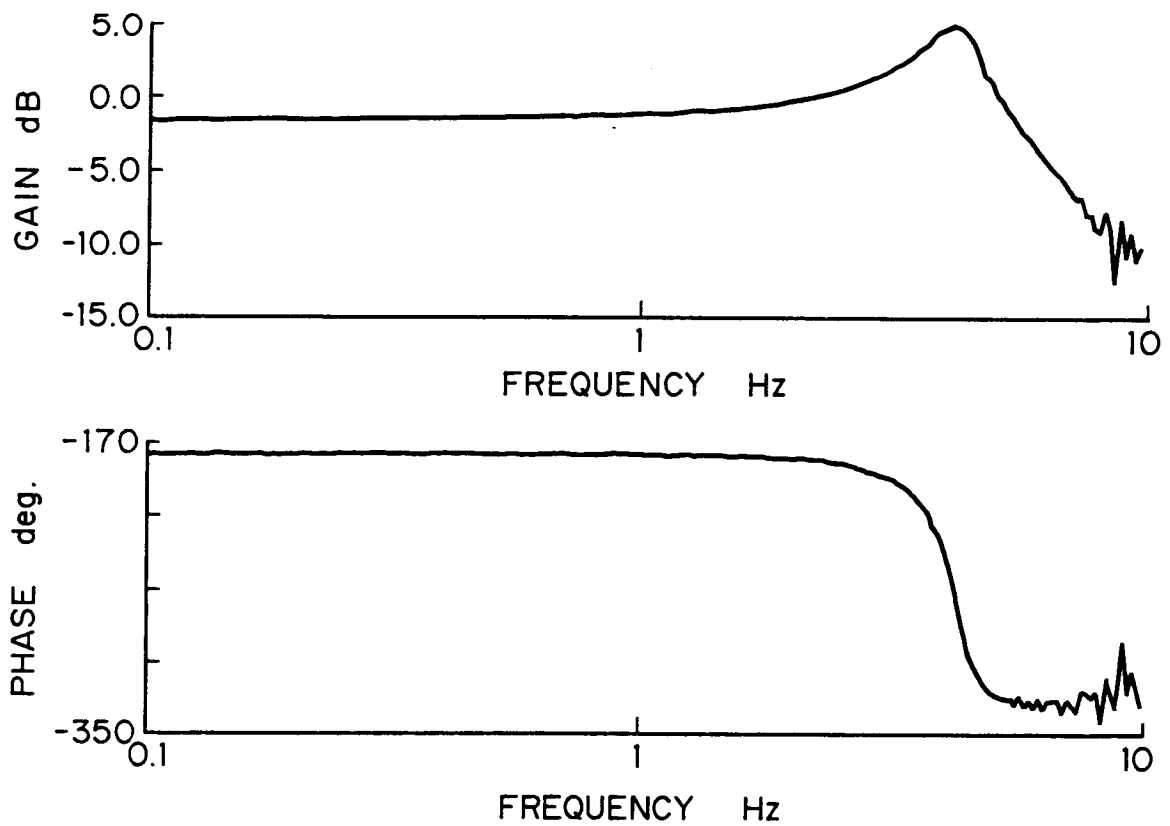


Figure 7 Frequency Response with Antenna Attached

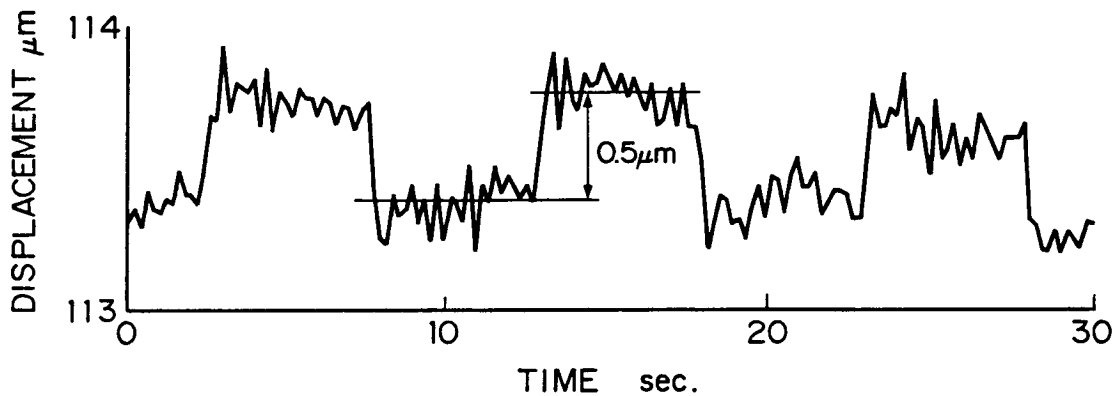
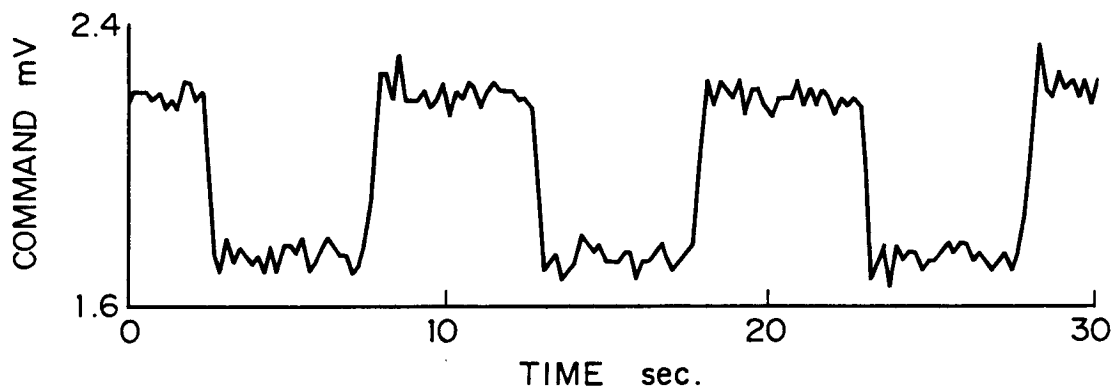


Figure 8 Resolution in z-axis with Antenna Attached

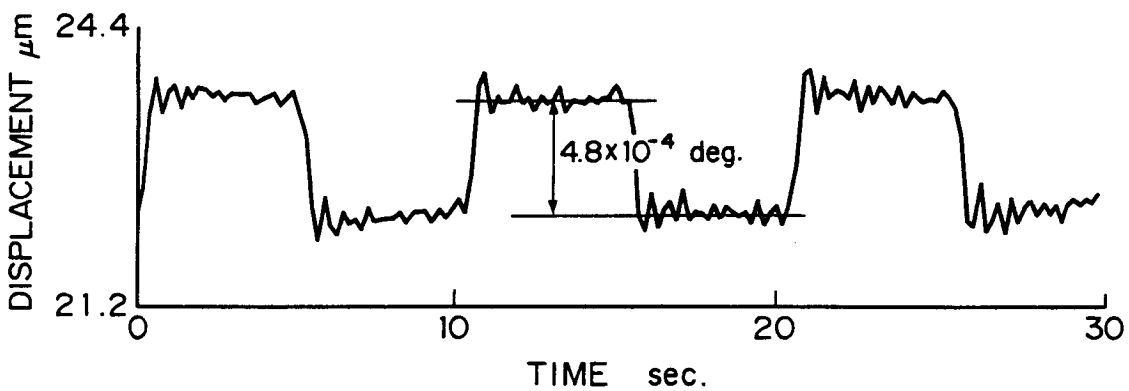
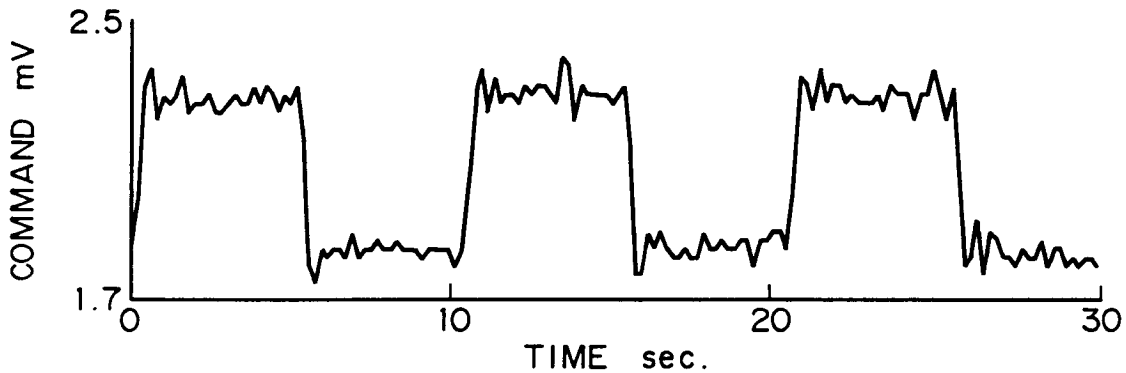


Figure 9 Resolution in Rotation around x-axis with Antenna Attached

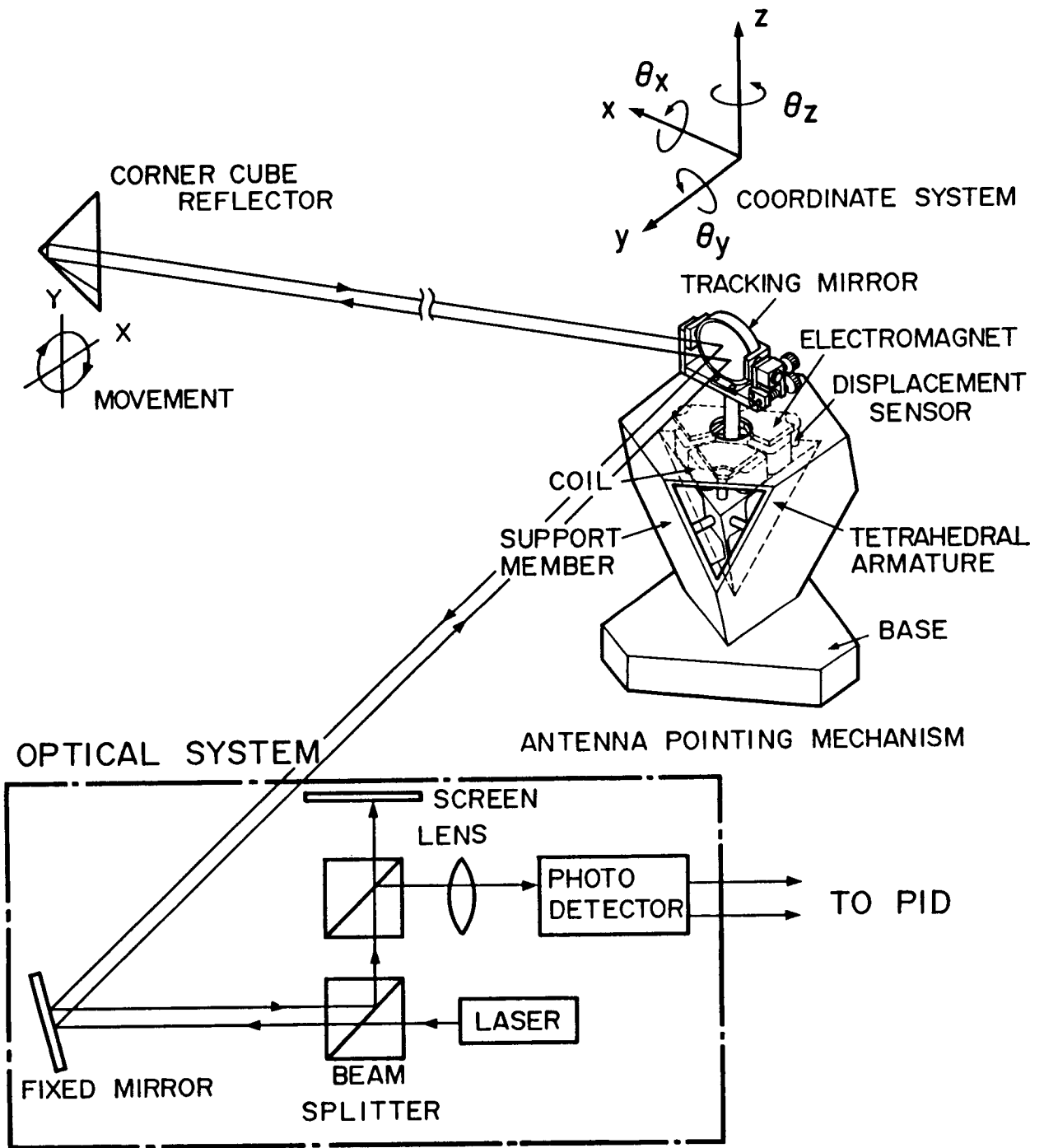


Figure 10 Laser Tracking System

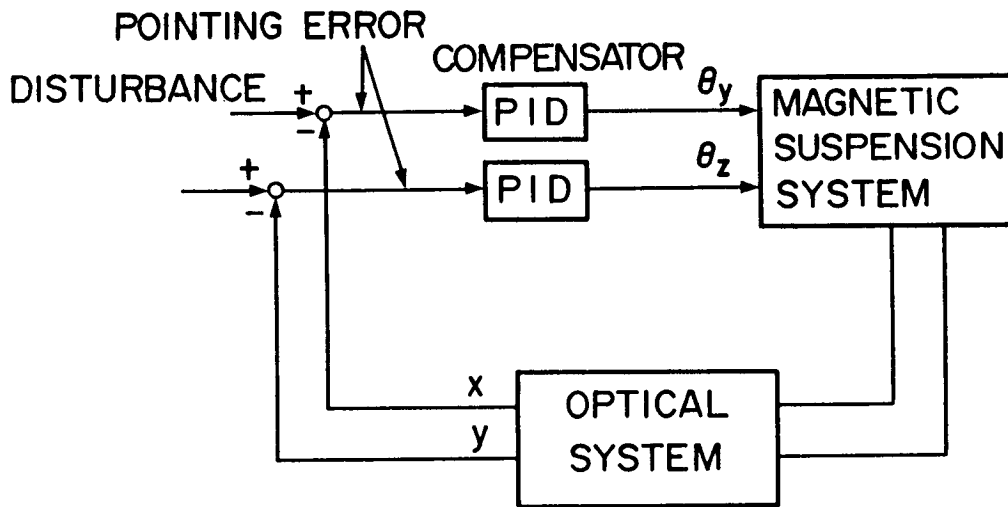


Figure 11 Pointing Closed Loop for Laser Tracking System

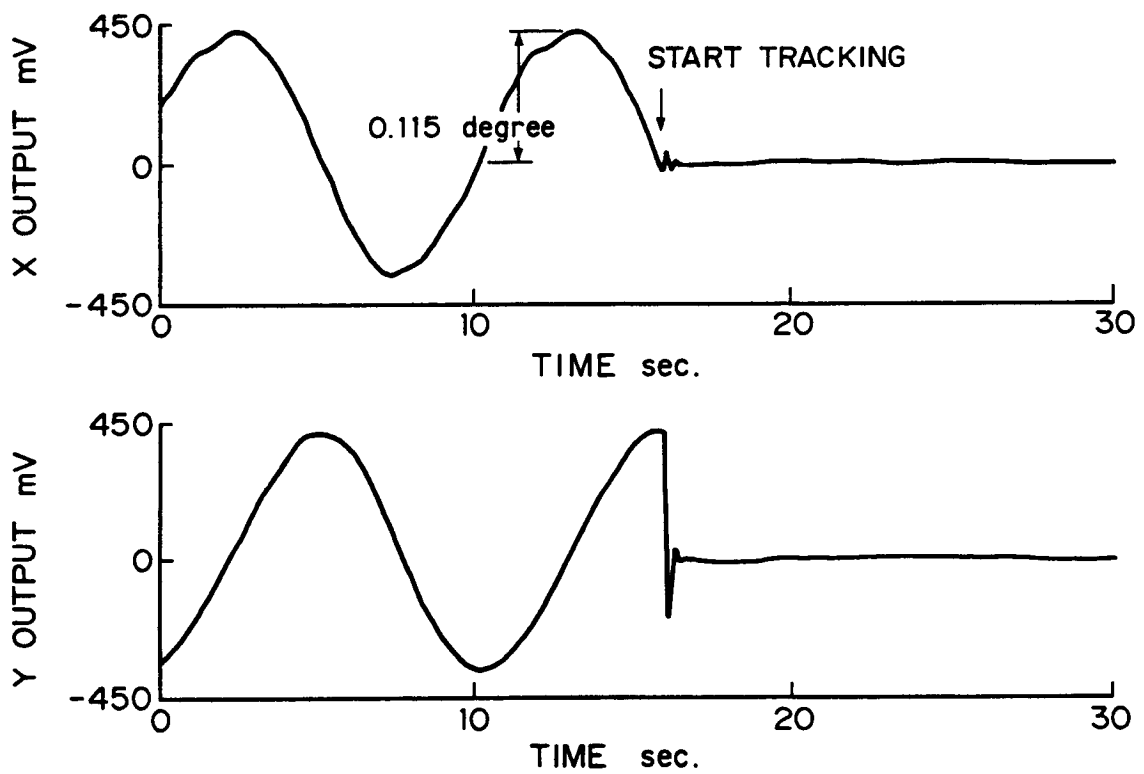


Figure 12 Tracking Characteristics  
(Two-dimensional photo detector outputs)